







# Ultrasonic Synthesis and Characterization of Zinc Pyrovanadate Nanostructures



O. A. Diyuk , Valery Zazhigalov , N. D. Shcherban , N. V. Diyuk ,  
V. V. Permyakov , S. M. Shcherbakov, L. S. Kuznetsova ,  
and M. M. Tsyba

**Abstract** The unique low temperature synthesis of zinc pyrovanadate from oxides was proposed.  $Zn_3V_2O_7(OH)_2 \cdot 2(H_2O)$  was synthesized by ultrasonic (US) method using ZnO and  $V_2O_5$  as raw materials. It was established using SEM and TEM methods that  $Zn_3V_2O_7(OH)_2 \cdot 2(H_2O)$  has the structure of nanosheets. The DTA method and XRD analysis showed the formation of the  $Zn_3V_2O_8$  phase after the removal of crystallization water from  $Zn_3V_2O_7(OH)_2 \cdot 2(H_2O)$ . Ultrasonic treatment of oxides as initial reagents allows obtaining  $Zn_3V_2O_8$  with the specific surface area of  $14 \text{ m}^2/\text{g}$ . For comparison,  $Zn_3V_2O_8$  was synthesized by solid-state (SS) synthesis from oxides. The properties of zinc pyrovanadate obtained by US synthesis and conventional SS synthesis were compared. The advantages of US method over conventional SS synthesis were noted.

---

O. A. Diyuk (✉) · V. Zazhigalov · L. S. Kuznetsova · M. M. Tsyba  
Institute for Sorption and Problems of Endoecology, National Academy of Sciences of Ukraine,  
General Naumov Street, 13, Kyiv 03164, Ukraine  
e-mail: [diyukhelen@ukr.net](mailto:diyukhelen@ukr.net)

V. Zazhigalov  
e-mail: [zazhigal@ispe.kiev.ua](mailto:zazhigal@ispe.kiev.ua)

N. D. Shcherban  
L.V. Pisarzhevsky Institute of Physical Chemistry, National Academy of Sciences of Ukraine, 31  
Pr. Nauky, Kyiv 03028, Ukraine  
e-mail: [nataliyalisenko@ukr.net](mailto:nataliyalisenko@ukr.net)

N. V. Diyuk  
Taras Shevchenko National University of Kyiv, 60 Volodymyrska Street, Kyiv 01033, Ukraine  
e-mail: [nvdiyuk@gmail.com](mailto:nvdiyuk@gmail.com)

V. V. Permyakov  
Institute of Geological Sciences, National Academy of Sciences of Ukraine, 55-B O.Gonchar Str.,  
Kyiv 01054, Ukraine

S. M. Shcherbakov  
M.G. Kholodny Institute of Botany, National Academy of Sciences of Ukraine, Tereshchenkivska  
Str., 2, Kyiv 01004, Ukraine  
e-mail: [sbarba@ukr.net](mailto:sbarba@ukr.net)

**Keywords** Zinc pyrovanadate ·  $\text{Zn}_3\text{V}_2\text{O}_8$  · Ultrasonic synthesis · Nanostructures

## 1 Introduction

Vanadium compounds are widely used in chemical industry as catalysts for the production of maleic acid, sulfuric acid, purification of industrial gases from  $\text{NO}_x$  [1, 2]. Moreover, vanadium compounds seem to be promising as novel potential drugs in the treatment of diabetes, atherosclerosis, and cancer [3, 4].

In the past few decades,  $\text{Zn}_3\text{V}_2\text{O}_8$  has attracted significant attention due to its unique properties and perspective for wide applications in industry, ecology, and medicine.

$\text{Zn}_3\text{V}_2\text{O}_7(\text{OH})_2 \cdot 2(\text{H}_2\text{O})$  and  $\text{Zn}_3\text{V}_2\text{O}_8$  are considered to be perspective for the creation of photoluminescence materials and can be used as a phosphor for white light emitting diodes [5].  $\text{Zn}_3\text{V}_2\text{O}_8$  with nanosheet structure demonstrates high performance as an anode material for lithium-ion batteries with good rate capacity, high cycling stability, and excellent discharge capacity as reported in [6]. Moreover, the zinc pyrovanadate nanowires show significantly improved electrochemical performance as an intercalation cathode for an aqueous zinc-ion battery [7]. It can be used for effective catalytic delignification and fractionation of lignocellulosic biomass [8], selective oxidation of sugars to carboxylic acids [9], and as photocatalysts [10–12]. It can be also applied as material for the sensing electrode to detect acetone (to 100 ppm) [13] and as material for an ethanol gas sensor [14].

However,  $\text{Zn}_3\text{V}_2\text{O}_8$  is usually obtained from soluble salts by a co-precipitation method [6, 11, 12, 15, 16] or from oxides by solid-state synthesis [10, 11, 17–20]. Both of these methods are not eco-friendly and require a long time. Usually for the obtaining  $\text{Zn}_3\text{V}_2\text{O}_7(\text{OH})_2 \cdot 2(\text{H}_2\text{O})$  with subsequent formation of  $\text{Zn}_3\text{V}_2\text{O}_8$ , typical synthesis from soluble salts is applied. The salts,  $\text{Zn}(\text{NO}_3)_2 \cdot 6\text{H}_2\text{O}$  and  $\text{NH}_4\text{VO}_3$ , are used more often for the synthesis of  $\text{Zn}_3\text{V}_2\text{O}_7(\text{OH})_2 \cdot 2(\text{H}_2\text{O})$  [13, 15, 16, 21, 22].  $\text{ZnCl}_2$  or  $\text{ZnSO}_4$  is used less often [6, 12, 23] but for all the experiments the molar ratio of  $\text{Zn}/\text{V} = 3:2$  was used. However, using highly diluted solutions due to the low solubility of  $\text{NH}_4\text{VO}_3$  should be noted. In addition, after the synthesis, the product must be washed several times to remove by-products. The superiority of this synthesis is possible formation of 2D nanosheets [6, 15] or 3D microspheres [11, 15] or even nanobelts [11, 16] structures of  $\text{Zn}_3\text{V}_2\text{O}_7(\text{OH})_2 \cdot 2(\text{H}_2\text{O})$ . The most of these references mention the use of an autoclave for the successful synthesis [6, 11, 16, 21, 23, 24]. An alternative is a solid-state method of syntheses leading to the direct formation of  $\text{Zn}_3\text{V}_2\text{O}_8$ . However, this method results in the formation of  $\text{Zn}_3\text{V}_2\text{O}_8$  with the grain shape possessing low  $S_{\text{BET}}$  of ca.  $0.5 \text{ m}^2/\text{g}$  [5]. Only conventional SS synthesis as the way to the formation of  $\text{Zn}_3\text{V}_2\text{O}_8$  from oxides was described in scientific literature. Although the SS synthesis can lead to the complete transformation of starting reagents without any pollution by by-products, it is impossible to obtain nanostructures by this method.

Therefore, the first method requires a lot of water for washing while the second one demands high temperature and doesn't lead to the formation of nanostructures. The possibility of the formation of zinc pyrovanadate from oxides under ultrasonic treatment has been studied in the current work. In addition, zinc pyrovanadate was synthesized by conventional solid-state method for comparison.

## 2 Experimental

### The samples preparation

Ultrasonic synthesis was carried out according to the procedure described in the literature [25] with some modifications. ZnO 2.86 g and V<sub>2</sub>O<sub>5</sub> 2.14 g powders (3:1 molar ratio) were mixed together, transferred into a beaker and de-ionized water (80 ml) was added. The weight ratio of initial oxides/water is 1/16. Ultrasonic treatment (UST) of the oxides mixture was carried out for 40 min at room temperature using an UZDN-A ultrasonic dispersant operating in an acoustic cavitations mode at a frequency of 22 kHz. A yellow suspension was obtained. The resulting product was filtered off, dried in air at 100 °C, and labeled as ZnVO\_US\_100. The sample ZnVO\_US\_100 was calcined at 500 °C in an alumina crucible in air for 4 h and labeled as ZnVO\_US\_500.

Additionally, Zn<sub>3</sub>V<sub>2</sub>O<sub>8</sub> was synthesized by a conventional solid-state method according to the procedure used in [10] with some modifications. ZnO 2.86 g and V<sub>2</sub>O<sub>5</sub> 2.14 g powders (3:1 molar ratio of oxides) were grinded using an agate mortar for 3 min, then transferred in an alumina crucible and calcined at 600 °C in air for 5 h. Afterward, the sample was cooled and grinded again using an agate mortar for 3 min. Finally, the sample was calcined at 750 °C in air for 6 h and labeled as ZnVO\_SS.

### Characterization of the samples

To analyze the samples composition and morphology, a scanning electron microscope (SEM JSM6490 LV, JEOL, Japan) with an integrated system for electron microprobe analysis INCA Energy based on energy-dispersive and wavelength-dispersive spectrometers (EDS + WDS, OXFORD, UK) with HKL Channel system was used.

Transmission electron microscopy (TEM) JEM-1200 EX (JEOL, Japan) was applied to study the materials morphology.

Nitrogen ad(de)sorption isotherms at -196 °C were obtained on a Quantachrome NOVA-220e Gas Sorption Analyzer. Specific surface area S<sub>BET</sub> was estimated using the BET equation.

Thermogravimetric analysis (DTA/TG) was carried out on a Derivatograph-Q apparatus with a heating rate of 10 °C/min under air atmosphere from room temperature to 700 °C. The sample mass was 200 mg.

### 3 Results and Discussion

#### XRD

Figure 1a shows the X-ray diffraction (XRD) patterns of the initial oxides mixture: ZnO (JCPDS card no. 00-080-0075) and  $V_2O_5$  (JCPDS card no. 00-041-1426).

In XRD pattern of ZnVO\_US\_100 (Fig. 1b), all the reflexes can be attributed to hexagonal structure  $Zn_3V_2O_7(OH)_2 \cdot 2(H_2O)$  (JCPDS card no. 00-087-0417) indicating high sample purity and crystallinity. ZnVO\_US\_500 has the diffraction signals corresponded to  $Zn_3V_2O_8$  (JCPDS card no. 00-034-0378) (Fig. 1c). Any peaks from others phases were not detected in the XRD patterns both for ZnVO\_US\_100 and

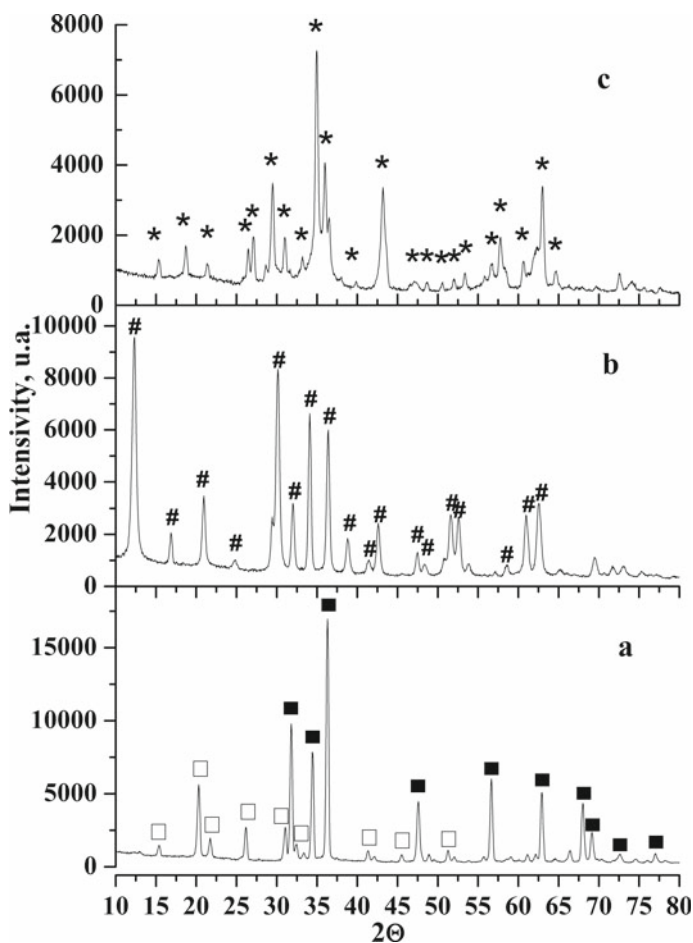
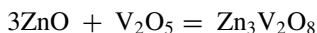
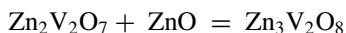
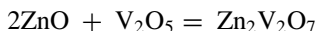


**Fig. 1** XRD patterns of **a** the initial mixture ZnO and  $V_2O_5$ , **b**  $Zn_3V_2O_7(OH)_2 \cdot 2(H_2O)$ , and **c**  $Zn_3V_2O_8$  where ■—ZnO, □— $V_2O_5$ , #— $Zn_3V_2O_7(OH)_2 \cdot 2(H_2O)$ , and \*— $Zn_3V_2O_8$

ZnVO\_US\_500 testifying the high purity of  $\text{Zn}_3\text{V}_2\text{O}_7(\text{OH})_2 \cdot 2(\text{H}_2\text{O})$  and  $\text{Zn}_3\text{V}_2\text{O}_8$  synthesized by ultrasonic treatment.

Figure 2 shows the XRD pattern of ZnVO\_SS. The most intensive peaks at  $2\Theta$ —15.4; 18.7; 21.4; 26.5; 27.1; 29.1; 31.0; 34.9; 36.0; 41.1; and 62.9 correspond to  $\text{Zn}_3\text{V}_2\text{O}_8$  as a main product. Moreover, the impurity phases of  $\text{Zn}_2\text{V}_2\text{O}_7$  (JCPDS card no. 00-070-1532) ( $2\Theta$ —16.7; 25.8; 28.64; 33.6; 40.6; and 42.2) and  $\text{ZnO}$  ( $2\Theta$ —31.7) were registered. It should be noted not long synthesis time (11 h) in our case compared to the conventional synthesis in other references [17–19]. Based on the XRD data, the following reactions can be assumed:



The synthesis of pyrovanadates by SS method usually is long-term and requires high temperatures. Therefore, the authors [11] synthesized vanadates by SS method during 1 week at  $T = 797^\circ\text{C}$  (XRD pattern was not shown; also there is no information about the impurities). In [10], synthesis was carried out during 60 h, and authors failed to synthesize pure  $\text{Zn}_3\text{V}_2\text{O}_8$  phase. The XRD patterns of their final product except  $\text{Zn}_3\text{V}_2\text{O}_8$  also have several peaks corresponded to a little amount of impurity phase (the impurity phase was not identified). Kurzawa et al. [20] investigated  $\text{V}_2\text{O}_5$ – $\text{ZnO}$  system and corresponding phase diagram. It was pointed out that the molar ZnO to

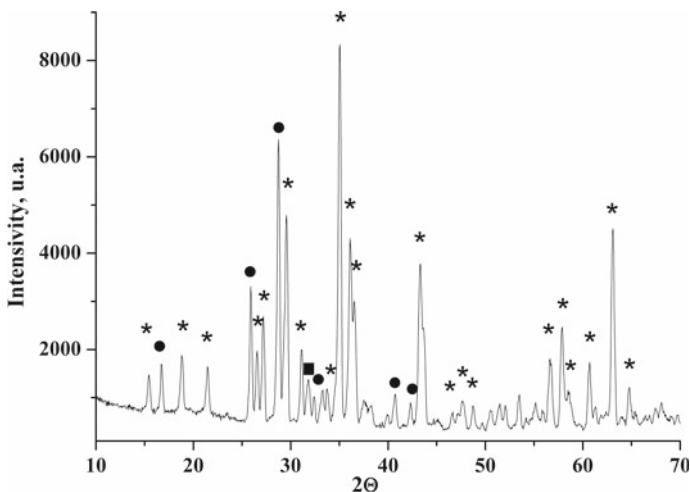
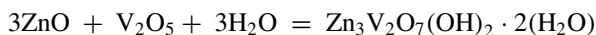


**Fig. 2** XRD patterns of  $\text{Zn}_3\text{V}_2\text{O}_8$  synthesized by solid-state synthesis from  $\text{ZnO}$  and  $\text{V}_2\text{O}_5$ : \*— $\text{Zn}_3\text{V}_2\text{O}_8$ , ●— $\text{Zn}_2\text{V}_2\text{O}_7$ , ■— $\text{ZnO}$

$V_2O_5$  ratio of 3:1 led to the formation of both  $Zn_3V_2O_8$  as  $Zn_2V_2O_7$  phases. It should be noted that the traditional solid-state synthesis of salts from oxides often leads to the formation of the main product with some amount of impurity phases [6, 25]. Comparison of the X-ray diffraction patterns of the product obtained as a result of ultrasonic and solvothermal synthesis allows to make an assumption about the key role of water in the formation of zinc pyrovanadate salt from oxides. And the key product is exactly zinc pyrovanadate crystal hydrate:



The absence of any impurity phases in the X-ray diffraction patterns of both ZnVO\_US\_100 and ZnVO\_US\_500 (Fig. 1b, c) also makes it possible to assume the formation of pure  $Zn_3V_2O_7(OH)_2$  phase with the subsequent transformation into pure  $Zn_3V_2O_8$  phase.

### SEM

SEM image of ZnVO\_US\_100 is shown in Fig. 3. Morphology of ZnVO\_US\_100 has a typical overall view for  $Zn_3V_2O_7(OH)_2 \cdot 2(H_2O)$  obtained by a conventional coprecipitate method [6, 9, 26]. Uniform size distribution of the particles in the sample is observed. The sample consists of nanoparticles in the form of nanosheets, each of which has a flat size of 0.1–1  $\mu\text{m}$  and a thickness of 10–40 nm. The data of energy-dispersive X-ray spectroscopy (determined at four different points) demonstrate the uniform elements distribution in the sample (Table 1). The data of SEM and EDX are in a good agreement with the XRD data (Fig. 1a) and confirm complete oxides conversion to  $Zn_3V_2O_7(OH)_2 \cdot 2(H_2O)$ .

### TEM

The TEM images of the initial oxides  $V_2O_5$  and ZnO used for the preparation of zinc vanadate by both ultrasonic and solid-state methods are presented in Fig. 4a, b,

**Fig. 3** SEM image of  $Zn_3V_2O_7(OH)_2 \cdot 2(H_2O)$

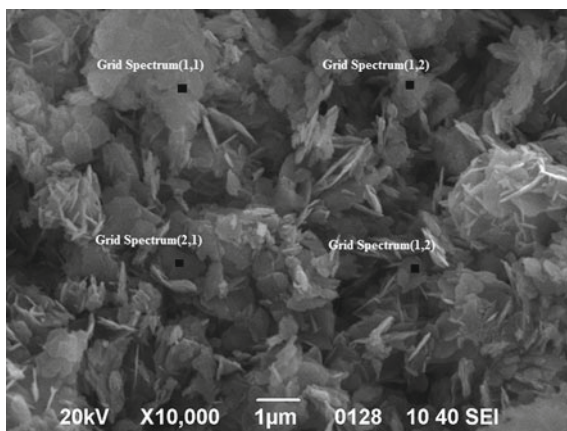


**Table 1** The results of energy-dispersive X-ray spectroscopy for ZnVO\_US\_100<sup>a</sup>

Spectrum	V	Zn	O
Grid Spectrum(1,1)	14.83	24.05	61.12
Grid Spectrum(2,1)	14.21	25.13	60.66
Grid Spectrum(1,2)	14.84	24.04	61.13
Grid Spectrum(2,2)	15.12	23.55	61.34
Mean	14.75	24.19	61.06
Std. deviation	0.38	0.67	0.29

<sup>a</sup> (All results in atomic %)

respectively. Typical particle of  $\text{Zn}_3\text{V}_2\text{O}_7(\text{OH})_2 \cdot 2(\text{H}_2\text{O})$  is displayed in TEM image Fig. 5a, b. TEM images of  $\text{Zn}_3\text{V}_2\text{O}_7(\text{OH})_2 \cdot 2(\text{H}_2\text{O})$  don't contain the particles of the initials oxides (Fig. 4a, b) instead, the particles with sheet-like structure gathered in agglomerates can be observed. The size of the particle plane ranges from several nm to 1  $\mu\text{m}$ . The light color of the  $\text{Zn}_3\text{V}_2\text{O}_7(\text{OH})_2 \cdot 2(\text{H}_2\text{O})$  particles indicate their small thickness. This is in a good agreement with the literature data about the sheet-like particles of  $\text{Zn}_3\text{V}_2\text{O}_7(\text{OH})_2 \cdot 2(\text{H}_2\text{O})$  obtained by a co-precipitation method [6, 11]. In addition, some amount of particles with hexagonal structure is present in TEM images. As known,  $\text{Zn}_3\text{V}_2\text{O}_7(\text{OH})_2 \cdot 2(\text{H}_2\text{O})$  crystallizes in the hexagonal space group P-6 [6, 11, 24].

### Specific surface area

The data of nitrogen ad(de)sorption (Fig. 6) show that the sample  $\text{Zn}_3\text{V}_2\text{O}_7$  obtained by a solid-state reaction is characterized by the low specific surface area ( $S_{\text{BET}}$  within 1  $\text{m}^2\text{g}^{-1}$ ) while the sample obtained by an US method have higher specific surface area ( $S_{\text{BET}}$  ca. 14  $\text{m}^2\text{g}^{-1}$ ), and ad(de)sorption isotherm has hysteresis in a wide area of relative nitrogen pressure indicating the presence of mesopores with different sizes.

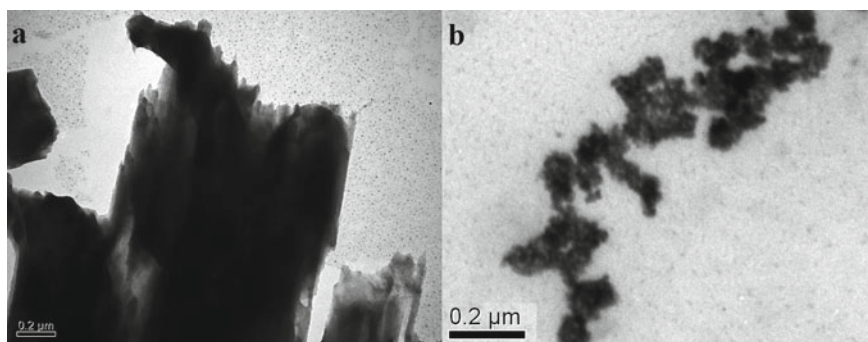


**Fig. 4** TEM images of the initial oxides **a**  $\text{V}_2\text{O}_5$  and **b**  $\text{ZnO}$

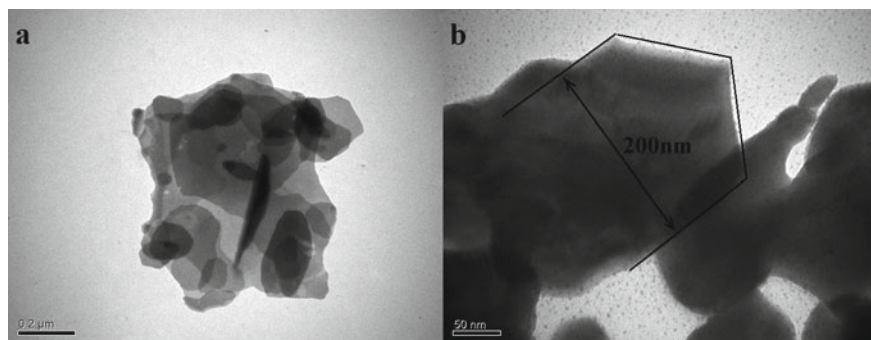


Fig. 5 TEM images of ZnVO\_US\_100

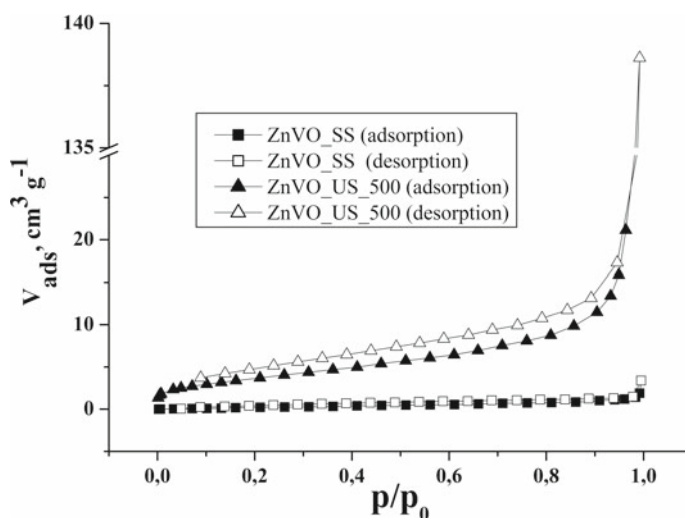


Fig. 6 Nitrogen ad(de)sorption isotherms (77 K) for  $\text{Zn}_3\text{V}_2\text{O}_8$  synthesized by the solid-state method and  $\text{Zn}_3\text{V}_2\text{O}_8$  synthesized by the ultrasonic method

## DTA

The thermal stability of  $\text{Zn}_3\text{V}_2\text{O}_7(\text{OH})_2 \cdot 2(\text{H}_2\text{O})$  was studied using DTA in air (Fig. 7). The TG curve has total weight loss of about 12.73% in an interval from 60 to 350 °C. The DTA curve has two endothermic peaks at 164 °C and 267 °C, being agreed well with weight loss on the TG curve. The removal of water of crystallization and coordinated water corresponds to the weight loss of 11.27%:  $\text{Zn}_3\text{V}_2\text{O}_7(\text{OH})_2 \cdot 2(\text{H}_2\text{O}) = \text{Zn}_3\text{V}_2\text{O}_8 + 3\text{H}_2\text{O}$ . Other 1.46% of weight loss can be explained by losing water adsorbed in the pore or on the surface. Published TG and DTA data for  $\text{Zn}_3\text{V}_2\text{O}_7(\text{OH})_2 \cdot 2(\text{H}_2\text{O})$  are contradictory. The maximum of the first endothermic peak is located at 163 °C well corresponding to [11]. Next endothermic peak is



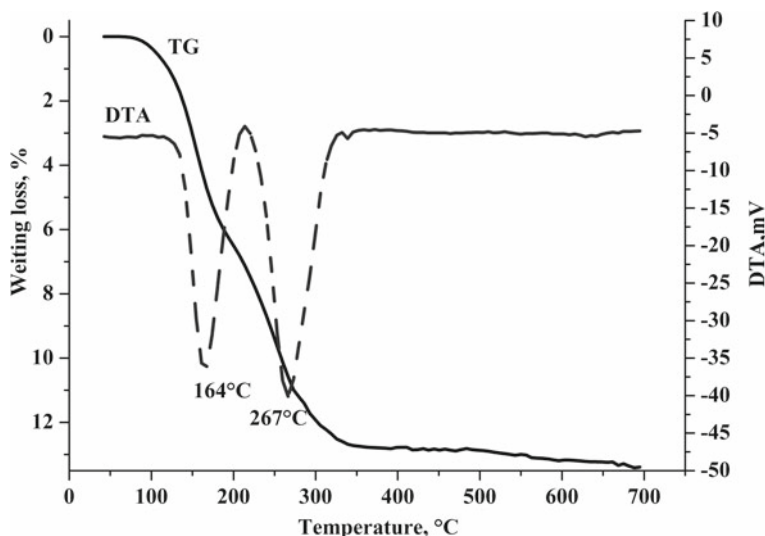


Fig. 7 TG and DTA analysis of  $\text{Zn}_3\text{V}_2\text{O}_7(\text{OH})_2 \cdot 2(\text{H}_2\text{O})$

located at 267 °C being more similar to the data described in [27]. Moreover, DTA curves presented in [11, 27] have exothermic peak at 452 °C and 550 °C, respectively. However, in our case, no exothermic peak in DTA curves was observed as well as in [15]. Such differences in the location of the maxima of endothermic peaks can be explained by the differences in the synthesis or TG and DTA analysis conditions.

Additionally, TG and DTA of the initial mixture of oxides were carried out, but no thermodynamic effects and weight loss were observed.

## 4 Conclusions

In summary, a facile, eco-friendly method of synthesis of  $\text{Zn}_3\text{V}_2\text{O}_7(\text{OH})_2 \cdot 2(\text{H}_2\text{O})$  followed by the formation of pure  $\text{Zn}_3\text{V}_2\text{O}_8$  phase was proposed. This approach in contrast to conventional co-precipitation synthesis doesn't require a lot of water for washing from polluting ions. The advantages of the US synthesis compared to the conventional SS synthesis are lower duration and temperature, as well as the formation of pure  $\text{Zn}_3\text{V}_2\text{O}_7(\text{OH})_2 \cdot 2(\text{H}_2\text{O})$  phase further transformed into pure  $\text{Zn}_3\text{V}_2\text{O}_8$  phase. Moreover, US synthesis allows obtain samples with nanosheet structures and high  $S_{\text{BET}}$ . Thus, the ultrasonic method is much more environmentally friendly than other traditional methods of synthesis.

**Acknowledgements** This work was financially supported by NASU Program "New functional substances and materials of chemical production" (project 13-21).

## References

1. Putluru SSR, Schill L, Godiksen A, Poreddy R, Mossin S, Jensen AD, Fehrmann R (2016) Promoted  $V_2O_5/TiO_2$  catalysts for selective catalytic reduction of NO with  $NH_3$  at low temperatures. *Appl Catal B* 183:282–290. <https://doi.org/10.1016/j.apcatb.2015.10.044>
2. Zazhigalov VA, Diyuk EA, Sidorchuk VV (2014) Development of VPO catalysts supported on mesoporous modified material based on an aerosol gel. *Kinet Catal* 55(3):399–408. <https://doi.org/10.1134/S002315840904017X>
3. Pessoa JC, Etcheverry S (2015) Vanadium compounds in medicine. *Coordination Chem Rev* 301–302:24–48. <https://doi.org/10.1016/j.ccr.2014.12.002>
4. Semiz S (2022) Vanadium as potential therapeutic agent for COVID-19: A focus on its antiviral, antiinflammatory, and antihyperglycemic effects. *J Trace Elem Med Biol* 69:126887. <https://doi.org/10.1016/j.jtemb.2021.126887>
5. Qian T, Fan B, Wang H, Zhu S (2019) Structure and luminescence properties of  $Zn_3V_2O_8$  yellow phosphor for white light emitting diodes. *Chem Phys Lett* 715:34–39. <https://doi.org/10.1016/j.cplett.2018.11.022>
6. Gan L, Deng D, Zhang Y, Li G, Wang X, Jiang L, Wang C (2014)  $Zn_3V_2O_8$  hexagon nanosheets: a high-performance anode material for lithium-ion batteries. *J Mater Chem A* 2:2461–2466. <https://doi.org/10.1039/C3TA14242F>
7. Xia C, Guo J, Lei Y, Liang H, Zhao C, Alshareef H (2017) Rechargeable aqueous Zinc-Ion battery based on porous framework Zinc pyrovanadate intercalation cathode. *Adv Mater* 1705580. <https://doi.org/10.1002/adma.201705580>
8. Khallouk K, Solhy A, Kherbeche A, Dubreucq E, Kouisni L, Barakat A (2020) Effective catalytic delignification and fractionation of lignocellulosic biomass in water over  $Zn_3V_2O_8$  mixed oxide. *ACS Omega* 5(1):304–316. <https://doi.org/10.1021/acsomega.9b02159>
9. Khallouk K, Solhy A, Idrissi N, Flaud V, Kherbeche A, Barakat A (2020) Microwave-assisted selective oxidation of sugars to carboxylic acids derivatives in water over zinc-vanadium mixed oxide. *Chem Eng J* 385:123914. <https://doi.org/10.1016/j.cej.2019.123914>
10. Wang D, Tang J, Zou Z, Ye J (2005) Photophysical and photocatalytic properties of a new series of visible-light-driven photocatalysts  $M_3V_2O_8$  ( $M = Mg, Ni, Zn$ ). *Chem Mater* 17:5177–5182. <https://doi.org/10.1021/cm051016x>
11. Shi R, Wang Y, Zhou F, Zhu Y (2011)  $Zn_3V_2O_7(OH)_2(H_2O)_2$  and  $Zn_3V_2O_8$  nanostructures: controlled fabrication and photocatalytic performance. *J Mater Chem* 21:6313–6320. <https://doi.org/10.1039/C0JM04451B>
12. Mondal C, Ganguly M, Sinha AK, Pal J, Sahoo R, Pal T (2013) Robust cubooctahedron  $Zn_3V_2O_8$  in gram quantity: a material for photocatalytic dye degradation in water. *Cryst Eng Comm* 15:6745–6751. <https://doi.org/10.1039/C3CE40852C>
13. Liu F, Guan Y, Sun R, Liang X, Sun P, Liu F, Lu G (2015) Mixed potential type acetone sensor using stabilized zirconia and  $M_3V_2O_8$  ( $M: Zn, Co$  and  $Ni$ ) sensing electrode. *Sens Actuat B* 221:673–680. <https://doi.org/10.1016/j.snb.2015.07.023>
14. Hua K, Cui M, Luo Z, Fang D, Bao R, Qi Q, Yi J, Sun B, Chen C (2019) Fabrication of Zinc pyrovanadate ( $Zn_3(OH)_2V_2O_7 \cdot 2H_2O$ ) nanosheet spheres as an ethanol gas sensor. *J Alloy Compd* 801:581–588. <https://doi.org/10.1016/j.jallcom.2019.06.015>
15. Zhang SY, Xiao X, Lu M, Li ZQ (2013)  $Zn_3V_2O_7(OH)_2 \cdot 2H_2O$  and  $Zn_3(VO_4)_2$  3D microspheres as anode materials for lithium-ion batteries. *J Mater Sci* 48:3679–3685. <https://doi.org/10.1007/s10853-013-7164-5>
16. Zhang S, Lei N, Ma W, Zhang Z, Sun Z, Wang Y (2014) Fabrication of ultralong  $Zn_3V_2O_7(OH)_2 \cdot 2H_2O$  nanobelts and its application in lithium-ion batteries. *Mat Lett* 129:91–94. <https://doi.org/10.1016/j.matlet.2014.05.047>
17. Gopal R, Calvo C (1971) Crystal structure of  $\alpha$ - $Zn_3(VO_4)_2$ . *Can J Chem* 49:3056–3059. <https://doi.org/10.1139/v71-510>
18. Clark GM, Pick AN (1975) DTA study of the reactions of  $V_2O_5$  with metal (II) oxides. *J Therm Anal* 7:289–300. <https://doi.org/10.1007/BF01911939>

19. Nord AG, Stefanidis T (1985) Crystal chemistry of  $a-(Zn, M)_2V_2O_7$  solid solutions correlation between preference for five-coordination and extension of solid solubility. *Mat Res Bull* 20:845–851. [https://doi.org/10.1016/0025-5408\(85\)90064-9](https://doi.org/10.1016/0025-5408(85)90064-9)
20. Kurzawa M, Rychlowska-Himmel I, Bosacka M, Blonska-Tabero A (2001) Reinvestigation of phase equilibria in the  $V_2O_5$ –ZnO system. *J Therm Anal Calorim* 64:1113–1119. <https://doi.org/10.1023/A:1011524424682>
21. Yang G, Li S, Wu M, Wang C (2016) Zinc pyrovanadate nanosheet of atomic thickness: excellent li-storage properties and investigation of electrochemical mechanism. *J Mater Chem A* 4:10974–10985. <https://doi.org/10.1039/C6TA02782B>
22. Mazloom F, Masjedi-Arani M, Salavati-Niasari M (2017) Rapid and solvent-free solid-state synthesis and characterization of  $Zn_3V_2O_8$  nanostructures and their phenol red aqueous solution photodegradation. *Solid State Sci* 70:101–109. <https://doi.org/10.1016/j.solidstatesciences.2017.06.013>
23. Low WH, Khiew PS, Lim SS, Siong CW, Chia CH, Ezeigwe ER (2019) Facile synthesis of graphene- $Zn_3V_2O_8$  nanocomposite as a high performance electrode material for symmetric supercapacitor. *J Alloy Compd* 784:847–858. <https://doi.org/10.1016/j.jallcom.2019.01.137>
24. Bayat A, Mahjoub AR, Amini MM (2018) Optical and magnetic properties of zinc vanadates: synthetic design of colloidal  $Zn_3V_2O_7(OH)_2(H_2O)_2$ ,  $ZnV_2O_4$  and  $Zn_3V_2O_8$  nanostructures. *J Mater Sci: Mater Electron* 29:2915–2926. <https://doi.org/10.1007/s10854-017-8222-6>
25. Diyuk OA, Zazhigalov VA, Shcherban ND, Permyakov VV, Diyuk NV, Shcherbakov SM, Sachukl OV, Dulian P (2021) Kinetics of  $ZnMoO_4 \cdot 0.8H_2O$  and  $\alpha$ - $ZnMoO_4$  formation at ultrasonic treatment of ZnO and  $MoO_3$  mixture. In: Fesenko O, Yatsenko L (eds) *Nanocomposites, nanostructures, and their applications*. Springer Proceedings in Physics book series, vol 263, 87–101. [https://doi.org/10.1007/978-3-030-74741-1\\_6](https://doi.org/10.1007/978-3-030-74741-1_6)
26. Luo J, Ning X, Zhan L, Zhou X (2021) Facile construction of a fascinating Z-scheme  $AgI/Zn_3V_2O_8$  photocatalyst for the photocatalytic degradation of tetracycline under visible light irradiation. *Sep Purif Technol* 255:117691. <https://doi.org/10.1016/j.seppur.2020.117691>
27. Hoyos DA, Echavarria A, Saldarriaga C (2001) Synthesis and structure of a porous zinc vanadate,  $Zn_3(VO_4)_2 \cdot 3H_2O$ . *J Mater Sci* 36:5515–5518. <https://doi.org/10.1023/A:1012418706071>